An Artificial Neural Network-based Real Time DSS to Manage the Discharges of a Wastewater Treatment Plant and Reduce the Flooding Risk

Loris Francesco Termite[1], Emanuele Bonamente[2], Alberto Garinei[3,4], Daniele Bolpagni[5], Lorenzo Menculini[4], Marcello Marconi[3,4], Lorenzo Biondi[3,4], Andrea Chini[6] and Massimo Crespi[6]

[1]*K-Digitale S.r.l., Perugia, Italy*

[2]*Department of Engineering, University of Perugia, Perugia, Italy*

[3]*Department of Sustainability Engineering, Guglielmo Marconi University, Rome, Italy*

[4]*Idea-Re S.r.l., Perugia, Italy*

[5]*A2A Ciclo Idrico S.p.A., Brescia, Italy*

[6]*Radarmeteo S.r.l., Due Carrare (PD), Italy*

Keywords: Decision Support System, Artificial Neural Networks, Flood Management, Flood Forecasting, Smart Infrastructures.

Abstract: An approach for sewerage systems monitoring based on Artificial Neural Networks is presented as a feasible and reliable way of providing operators with a real-time Decision Support System that is able to predict critical events and suggest a proper mitigation strategy. A fully-working prototype was developed and tested on a sewerage system in the city of Brescia, Italy. The system is trained to forecast flows and water levels in critical points of the grid based on their measured values as well as rainfall data. When relying on observed rainfall only, key parameters can be predicted up to 60 minutes in advance, whereas including very-short-term Quantitative Precipitation Estimates – nowcasting – the time horizon can be extended further, up to 140 minutes in the current case study. Unlike classical hydraulic modelling, the proposed approach can be effectively used run-time as the execution is performed with a negligible computational cost, and it is suitable to increase safety measures in a Smart City context.

1 INTRODUCTION

In many urban scenarios, the management of wastewater is performed by combined sewer systems, collecting both storm water and black/greywater in order to send them to the wastewater treatment plant (WWTP). In case of intense rainfall events, the sewer discharge may reach its capacity limit and occasionally produce combined sewer overflow (CSO), leading to pollution risk. Moreover, excessive discharges of treated water may produce floods if the stage of the receiving bodies is already high due to rainfall. Specific structures – spillway gates, buffer tanks, pumps, etc – are designed to mitigate such occurrences. Clearly, an optimal intervention strategy during a critical event strongly relies on the accurate knowledge of the system status (water flows and levels, gate openings) and, possibly, the weather conditions (i.e. observed and expected rainfalls). The lack of a comprehensive monitoring and forecast network requires the operators to choose the intervention strategy by relying mostly on their experience. In such contexts, a decision support system (DSS) may represent a fundamental aid (Pereira et al., 2019).

DSSs are platforms dedicated to providing support to the human operator in deciding which operations to perform. Several examples are available in the literature for sewerage systems-related applications (Park and Kim, 2013; Rao, 2015), their focus being on the design, renovation, and upgrade of the physical system or on the offline reanalysis of past events in order to optimize future intervention strategies. Instead, the monitoring of sewerage networks using real-time data has been mainly focused on pollution emissions and concentrations (Rechdaoui-Guérin et al., 2018).

Termite, L., Bonamente, E., Garinei, A., Bolpagni, D., Menculini, L., Marconi, M., Biondi, L., Chini, A. and Crespi, M.
An Artificial Neural Network-based Real Time DSS to Manage the Discharges of a Wastewater Treatment Plant and Reduce the Flooding Risk.
DOI: 10.5220/0010396500150026
In *Proceedings of the 10th International Conference on Smart Cities and Green ICT Systems (SMARTGREENS 2021)*, pages 15-26
ISBN: 978-989-758-512-8

In recent years, smart network monitoring began to find development and applications. The advances in technology can be exploited by municipalities, utilities, and related organizations to implement smart data infrastructure for wet weather control. More specifically, advanced monitoring data are used to support wet weather control and decision-making in real time or near real time. The United States Environmental Protection Agency defines smart infrastructures as "the integration of emerging and advanced technology to enhance the collection, storage, and/or reanalysis of water-related data", making use of "hardware, communication and management analytics to provide real and tangible benefits to utilities", as "maximizing existing infrastructure and optimizing operations and responses to be proactive, not reactive" (US EPA, 2018). Smart infrastructures are generally implemented in connection with a supervisory control and data acquisition (SCADA) system. Their main objective is usually the real-time monitoring of CSO's flow rates and effluent level, in order to assess potential flooding and pollution incidents and to support real-time or quasi real-time decision making about actions to be taken (Botturi et al., 2020).

However, to the best of the authors' knowledge – with particular reference to the Italian territory – the diffusion of smart infrastructures is still quite limited. Despite the presence of few studies aimed at reducing CSO through Real Time Control of gates and sluices (Carbone et al., 2014; Campisano et al., 2016), some issues are not addressed properly, as the potential risk of flooding due to excessive discharge of treated water from the WWTP to the receiving body. Most of real-world DSS implementations aimed at flood mitigation still rely on traditional hydraulic models and are often characterized by a high computational demand making them unsuitable for real-time usage. Sometimes such models proved to be outdated and are not resilient to climate change. Moreover, there is lack of use of very-short-term precipitation forecasts, which are crucial in case of high-intense and short-lasting rainfall events.

This paper presents a case study about the design of a DSS dedicated to WWTP management. It allows real-time monitoring of the system status through a network of ground-based meters and weather radars. It also includes a forecasting tool that provides additional information to help operators in planning manoeuvres, thanks to a methodology based on Artificial Intelligence – specifically Artificial Neural Networks (ANNs) (Maier et al., 2010) – estimating water levels and flows inside the network. ANNs are suitable tools for the purposes of this study, since they allow for a reduction in the input data variety – selecting only the most statistically significant in the input-output relation – and the non-use of parameters needed by traditional models, as for example the soil properties in rainfall-runoff modelling. Moreover, after being calibrated, their execution is immediate and perfectly matches the real-time requirements. They can also be easily updated, well facing possible changes in the real environment.

The aim of the implemented DSS is to give operators useful insights about the current status of the receiving water body in strategic locations, the potential CSO amount, the WWTP inflow, the current and recent rainfall and the estimated evolution of the strategic variables, collecting all data and showing them in a single User Interface, to eventually guide them to apply a proper risk mitigation strategy.

As regards rainfall information, the DSS also exploits high resolution very-short-term quantitative precipitation forecasting, also known as "nowcasting" (Wilson et al., 1998). Quantitative precipitation forecasting is performed by means of algorithms working on rainfall measures provided by weather radars (Bellon et al., 2010; Lee et al., 2010). It has been proved that radar-based nowcasting can give more reliable results than classic numerical weather prediction within a time horizon of 3-8 hours (Mandapaka et al., 2012), being therefore a valuable tool for real-time decision-making. In the present context, nowcasting is used to further extend the time horizon of ANNs predictions for hydraulic variables, allowing to manage the potential emergencies with a reasonable advance.

The designed DSS provides real-time monitoring of the hydraulic system status and – thanks to ANNs – predicts its future evolution. Once the model calibration has been performed, the ANNs algorithms consist in linear algebra operations on matrices which require negligible computational times, unlike more traditional hydraulic models that as of today require large computational times and computing resources (Clark et al., 2017).

2 METHODOLOGY

2.1 Description of the System Layout

The WWTP for which the DSS was developed collects the sewage and urban runoff in the city of Brescia (Italy) and its surrounding area, serving a total of 296.000 inhabitants over a 146 km^2 surface. Figure 1 shows the system layout.

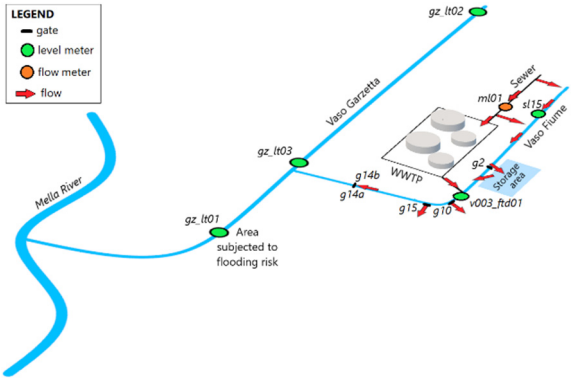

Figure 1: System layout.

An urban drainage channel named Vaso Fiume (VF) runs parallel to the final sewer collector, upstream the WWTP. When the sewer flow raises above a critical level, the excess is directed into the VF trough two lateral spillways, one located just before the WWTP and one a few km upstream. The VF also receives the treated wastewater. A bigger urban drainage channel, named Vaso Garzetta (VG), collects water from the VF approximately 2.4 km downstream and eventually flows into the Mella river after a 3.4 km path. The whole network of receiving water bodies is characterized by potential hydraulic risk in case of extreme rainfall events: over the last years urban flooding has occurred several times along the VG channel, in a critical location corresponding to the *gz_lt01* measuring point (approximately 1.7 km downstream the confluence with VF). In such circumstances, the water flowing from VF into VG should be constrained and the WWTP technicians must pay close attention in order to minimize the risk of flooding. To this aim, the VF channel is equipped with a series of inline or lateral gates, which can be used effectively for flood prevention. Two lateral gates (*g10* and *g15*), which are closed in standard conditions, can be gradually opened to direct the flow in the surrounding rural area, within environmental law limitations. A couple of paired inline gates (*g14a* and *g14b*), which are kept open in standard conditions, can be progressively closed to reduce, and in certain cases completely arrest, the VF flow into the VG. A storage area is also present next to the WWTP and is used to reduce the peak discharge into the VF: an inline gate (*g2*) can be partially closed in order to increase the upstream water level and activate a lateral spillway into the storage area.

The WWTP and the sewage network are managed by a leading multiutility society which has been playing much effort in Smart City projects over the last years. The wish of the WWTP managers was to have a tool able to assist them in taking proper decision especially when dealing with severe rainfall events. Indeed, prior to the development of the present DSS platform, the gate-opening strategy relied only on operator experience – based on information from the upstream *gz_lt02* meter – to foresee impending flood waves. Operators decided whether to use the storage area and to open lateral spillways in order to reduce the outflow towards the VG channel and prevent downstream overflows. However, the users lacked an interface allowing a thorough monitoring of the system status. In particular, information about forthcoming rainfall amounts, water levels and sewer flows was completely missing. In case of severe events, such an approach was not able to completely avoid risks.

In addition to the VG level at *gz_lt02*, particular attention is also devoted to the WWTP inlet (*ml01*), as treatment cycles can be optimized thanks to the presence of an internal buffer tank. Since during extreme events the flow at *ml01* may exceed the WWTP processing capacity, knowing this flow in advance can help to properly manage the internal operation of the plant. Therefore, the VG level at *gz_lt02* and the flow at *ml01* are key parameters to be monitored. Their expected values are forecasted by the ANNs developed for the DSS.

2.2 The Decision Support System

2.2.1 Data Acquisition

Prior to the DSS implementation, the acquired data (rainfall, levels, flows, gate openings) were collected in diverse databases and visualized in separate interfaces, preventing the WWTP operators from having a comprehensive view of the system status.

Rainfall data used to be provided only by six pluviometers within the catchment; for the purposes of the present study it was instead decided to also exploit advanced meteorological radar measurements. To this end, distributed rainfall measurements performed by radars were calibrated through the punctual pluviometer records, eventually obtaining reliable information in terms of both value accuracy and spatial variability. The resulting product has 1×1 km spatial resolution as in Panziera et al. (2011) and a 10-minutes time resolution.

The resulting integrated rainfall measurements were spatially averaged over the whole catchment to obtain a single value to be used as an input for the ANNs. Preliminary attempts demonstrated that distinguishing over rainfalls precipitated in different zones only makes water levels and flows forecasts

less stable and does not produce any significant improvement over using the mean areal rainfall.

The readout of each sensor was synchronized, the time step was fixed to 10 minutes, and a dedicated server was realized to host the system database containing all the records of measured data, computed quantities and final parameters.

2.2.2 ANNs Setup

Rainfall, *gz_lt02* level and *ml01* discharge data were made available for a period spanning from October 2016 to August 2018.

A set of four ANNs was set up, two predicting VG level variation and the other two predicting sewer flow variation.

The effect produced on target variables by rainfall is visible with a lag time that was found to vary between 30 minutes and 2 hours. Thus, it was decided to predict them up to 60 minutes beyond the last known rainfall information, whether measured or predicted.

More specifically, the ANN named ANN_{LS} (level/short-term) makes use of measured rainfalls only and provides *gz_lt02* level forecast up to 60 minutes; ANN_{LL} (level/long-term) uses also nowcasting up to +80 minutes, thus extending the forecast horizon to 140 minutes. Similarly, ANN_{FS} (flow/short-term) and ANN_{FL} (flow/long-term) forecast sewer discharge at *ml01*. ANN_{LS} and ANN_{LL} were trained and validated using 18 suitably trimmed rainfall events in the analysed period, corresponding to a total 1714 datapoints; ANN_{FS} and ANN_{FL} used 17 events, with 12057 datapoints. Due to the available data, the two samples refer to different sets of events. The higher number of datapoints used to train sewer-related ANNs depends on the fact that events were trimmed in larger chunks, because flows at *ml01* take longer to return to the unperturbed value after rainfalls with respect to levels at *gz_lt02*.

Measured rainfall inputs for ANN_{LS} and ANN_{LL} cover the antecedent 2-hours interval. This extension was considered appropriate, covering the whole range of observed lags. A longer period (six hours) was required for *ml01* forecast, due to the longer-lasting observed perturbation induced on the sewer collector by precipitation.

Rainfall measurements are updated every 10 minutes, while nowcasting is updated every 20 minutes due to computing limitations. This results in two different updating frequencies for short-term and long-term predictions, consistent with rainfall input updates. For convenience, the rainfall measurements provided to the ANNs are also aggregated in 20-minute bins, although updated every 10 minutes. Moreover, to keep track of the initial conditions, the current level/flow is also used as input.

For all the ANNs, the targets are the level/flow variations induced by rainfall, with respect to the current value, evaluated on a 10-minute basis. Thus, at every execution, ANN_{LS} and ANN_{FS} produce six outputs (10-minute bins from +10 to +60), while ANN_{LL} and ANN_{FL} produce fourteen outputs (10-minute bins from +10 to +140).

The expected levels are obtained by the algebraic sum of current values and predicted variations. The expected flows calculation needs an additional term to be considered in the sum, i.e. the characteristic daily modulation of sewer discharge. Thus, the average flow profile at *ml01* was obtained disregarding rainy days and was found to lie in the range 0.5-1.2 m^3/s (Figure 2), then the corresponding 144 average flow variations – on a 10-minute basis from 0:00 to 23:50 – were computed.

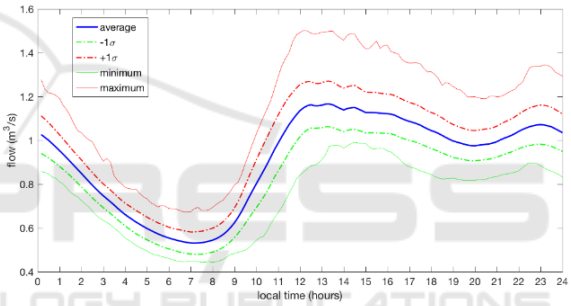

Figure 2: Average *ml01* profile during dry days (blue line).

The Multilayer Perceptron structure was chosen to build the ANNs, that were developed in a MATLAB environment. After trial-and-error attempts, the layout was chosen so that all the ANNs share a common structure, with a 20-nodes single hidden layer connecting the input and output layers. All the inputs and targets were normalized between 0 and 1. A logistic activation function is used in the hidden layer, and a linear activation function is used in the output layer to produce the results. It is customary in Machine Learning to use three different sets of data, namely the calibration, validation and testing set: the calibration and validation set are used to train the networks, with the first used to fix weights and biases and the latter to adjust the hyperparameters; the testing set is used to test the ANNs performance on unseen data. However, due to some uncertainties in the available data, and since the aim of this study was not to explore ANNs' theory but instead it was necessary to exploit as much data as possible to build a ready-to-use product, it was

decided to disregard the testing set. Therefore, the available datasets were split using the last four events (380 datapoints, i.e. 22.17% for level forecast; 2274 datapoints, i.e. 18.86% for flow forecast) for the validation set and the previous ones for the calibration set.

Weights and biases in the ANNs nodes were randomly initialized, and the Levenberg-Marquadt backpropagation algorithm was used to minimize the cost function, specifically the mean square error between the target/output pairs; the algorithm execution was imposed to stop if the validation error increased for 20 consecutive iterations. Since the training procedure outcome varies depending on the randomly generated initial parameters and on the chance of the training algorithm getting stuck in local minima, each ANN was trained 2000 times using the above-mentioned procedure, and the best-performing network was then selected.

Rather than considering the cost function, a more detailed multi-objective optimization was implemented to select the best performing ANNs, keeping in mind their final purpose, i.e. a correct and prompt forecast of the most severe events. Thus, for both level and flow, three threshold values were defined, i.e. 70, 100 and 140 cm at *gz_lt02* and 2.5, 3.5 and 4.5 m^3/s at *ml01*. Four objectives were defined to select the best performing ANNs.

1) The Nash-Sutcliffe Efficiency index (NSE) computed on actual network targets and outputs (normalized values). The optimization variable to be minimized is the subtracted ratio in the NSE definition:

$$NSE = 1 - \frac{\sum_{i=1}^{n}(O_i - S_i)^2}{\sum_{i=1}^{n}(O_i - \bar{O})^2} \quad (1)$$

where O_i are the observed values, $\bar{O}$ is their mean value and S_i are the simulated values. *NSE* is computed for each prediction horizon (10 minutes, 20 minutes, …etc.) and the objective is found from the mean of the computed values.

2) Maximum number of correct predictions of threshold values crossing. The optimization variable, to be minimized, is the ratio of missed predictions to observed crossings. It is computed for each alert level and the objective is set to the mean of the three computed values.

3) Minimum number of fake predictions (threshold crossing prediction not corresponding to observed crossing). The optimization variable, to be minimized, is the ratio of fake predictions to total predictions, either true or false. It is computed for each alert level and the objective is set to the mean of the three computed values.

4) Optimal prediction timing. Every time there is an observed threshold level crossing in the forecast time horizon after current timestamp and there is also a predicted crossing, the delay between the observed and predicted time of crossing is computed. The objective to minimize is the mean squared delay for all alert levels.

Objectives n.2 and n.3 vary between 0 and 1. In order to give objective n.1 the same range of variability, the upper boundary of the subtracted ratio was set to 1, as values greater than 1 would imply a non-acceptable performance and the related solution should be discarded. Objective n.4 was normalized between 0 and 1 with respect to its possible minimum and maximum values (i.e. 0 and 50 minutes for short-term predictions and 0 and 130 minutes for long-term predictions). In looking for the Pareto front of undominated solutions, the second and fourth objectives were given a weight triple than the others. This was mainly due to sewer management reasons. Among these points in the 4-D resulting spaces, the best performing combinations were selected as those with the minimum Euclidean norm and the corresponding sets of weights and biases matrices were used in the algorithms running in the DSS.

Since objectives n.2, n.3 and n.4 can be computed only on threshold crossings – and therefore on a small amount of data – the above-mentioned optimization procedure was performed on the whole available dataset, comprising both training and validation datapoints.

3 RESULTS

3.1 ANNs Performance

The multi-objective optimization led to the selection of the best performing ANNs. A first evaluation of their performance was made according to the objectives described in section 2.2.2. The obtained values are shown in Table 1. A better general performance of level prediction with respect to sewer discharge prediction can be noticed. Moreover, better predictions are obtained from ANNs exploiting nowcasting information.

Table 1: Results of the multi-objective optimization: values for the selected ANNs.

	OBJ 1	OBJ 2	OBJ 3	OBJ 4
ANN_{LS}	0.241	0.150	0.106	0.061
ANN_{LL}	0.128	0.137	0.039	0.037
ANN_{FS}	0.531	0.175	0.117	0.100
ANN_{FL}	0.412	0.201	0.069	0.083

Statistical analyses were performed on the results. For all the selected ANNs, the *NSE* index was calculated for each event and each forecasting horizon (+10 to +60 minutes or +10 to +140 minutes). Calibration values for ANN_{LS} – averaged on the 14 events in the set – range between 0.484 and 0.888, with higher values corresponding to shorter forecasting horizons. Similarly, average validation values are comprised between 0.294 and 0.906. ANN_{LL} gave *NSE* average values ranging between 0.301 and 0.601 for calibration events and between 0.103 and 0.903 for validation ones. The ranges of average *NSE* values are 0.987÷0.909 and 0.904÷0.989 for ANN_{FS} calibration and validation events, respectively. Finally, *NSE* average ranges for ANN_{FL} are 0.843÷0.986 (calibration) and 0.789÷0.988 (validation). As a term of comparison, Jeong et al. (2010) obtained *NSE* = 0.74 for calibration data and *NSE* = 0.63 for validation data when modelling stream flows in a small watershed using the SWAT tool. However, this kind of analysis does not give useful insights on the ANNs efficiency in the DSS and may even be misleading. Indeed, the main goal of a real-time DSS like as the one presented

Table 2: Performance of the selected ANNs in predicting threshold crossings. Values outside brackets refer to the whole dataset; values in brackets refer to calibration and validation sets, respectively.

		Threshold 1	Threshold 2	Threshold 3
ANN_{LS}	n. observed.	22 (17 / 5)	9 (6 / 3)	4 (2 / 2)
	n. predicted.	22 (17 / 5)	6 (4 / 2)	3 (2 / 1)
	predicted %	100.0 (100.0 / 100.0)	66.7 (66.67 / 66.67)	75.0 (100.0 / 50.0)
	a.w.t. (min)	36.8 (35.2 / 42.0)	25.0 (27.5 / 20.0)	33.3 (35.0 / 30.0)
	a.p.d. (min)	3.2 (3.6 / 2.0)	1.7 (0.0 / 5.0)	-3.3 (0.0 / -10.0)
	false alerts	10 (7 / 3)	1 (1 / 0)	0 (0 / 0)
ANN_{LL}	n. observed.	22 (17 / 5)	9 (6 / 3)	4 (2 / 2)
	n. predicted.	22 (17 / 5)	5 (3 / 2)	3 (2 / 1)
	predicted %	100.0 (100.0 / 100.0)	55.6 (50.0 / 66.67)	75.0 (100.0 / 50.0)
	a.w.t. (min)	97.7 (91.8 / 118.0)	116.0 (110.0 / 125.0)	113.3 (115.0 / 110.0)
	a.p.d. (min)	-7.3 (-5.9 / -12.0)	-10.0 (-3.3 / -20.0)	3.3 (0.0 / 10.0)
	false alerts	9 (6 / 3)	4 (2 / 2)	0 (0 / 0)
ANN_{FS}	n. observed.	56 (45 / 11)	11 (7 / 4)	2 (1 / 1)
	n. predicted.	34 (31 / 3)	7 (4 / 3)	2 (1 / 1)
	predicted %	60.7 (68.9 / 27.3)	64.7 (57.1 / 75.0)	100.0 (100.0 / 100.0)
	a.w.t. (min)	35.9 (36.4 / 30.0)	22.9 (22.5 / 23.3)	45.0 (30.0 / 60.0)
	a.p.d. (min)	0.0 (0.3 / -3.3)	5.7 (15.0 / -6.7)	5.0 (20.0 / -10.0)
	false alerts	16 (10 / 6)	2 (1 / 1)	0 (0 / 0)
ANN_{FL}	n. observed.	56 (45 / 11)	11 (7 / 4)	2 (1 / 1)
	n. predicted.	36 (32 / 4)	9 (5 / 4)	2 (1 / 1)
	predicted %	64.3 (71.1 / 36.4)	81.8 (71.4 / 100.0)	100.0 (100.0 / 100.0)
	a.w.t. (min)	71.4 (69.7 / 85.0)	73.3 (98.0 / 42.5)	100.0 (70.0 / 130.0)
	a.p.d. (min)	8.9 (8.4 / 12.5)	5.6 (2.0 / 5.0)	15.0 (30.0 / 0.0)
	false alerts	15 (5 / 10)	2 (2 / 0)	0 (0 / 0)

in this case study is to guarantee that accurate alerts are sent sufficiently in advance, allowing operators to act promptly. Therefore, the performances of the selected ANNs were also evaluated according to the metrics defined in Table 2 (please note that values outside brackets refer to the whole datasets, while first and second values in brackets refer to calibration and validation sets, respectively). For each ANN, the total number of observed crossings of the defined threshold values (70, 100 and 140 cm *at gz_lt02*; 2.5, 3.5 and 4.5 m^3/s at *ml01*) is displayed, along with the number of corresponding predictions and related percentages of correctly predicted crossings. Given the DSS updating frequency, observed crossings can be forecasted with an anticipation varying (with a 10-minute resolution) from 60 to 10 minutes for ANN_{LS} and ANN_{FS} and from 140 to 10 minutes for ANN_{LL} and ANN_{FL}. A crossing is considered predicted if it is signalled to occur at least once in the available forecasting horizon. Two other parameters that were evaluated are the average warning time (a.w.t. in Table 2), i.e. the mean anticipation corresponding to the first alert of impending crossing, and the average prediction delay (a.p.d. in Table 2), indicating the accuracy of the prediction timing. As an example, if the DSS first signals an impending crossing by warning that it will happen after 40 minutes, but the actual crossing is observed after 30 minutes, then the warning time is 30 minutes and the prediction delay is 10 minutes. Finally, the number of false alerts is shown. In contrast to correct crossing predictions, an alert is considered false if there is no actual crossing at any time step of the forecasting horizon.

From Table 2 it is possible to see that all the ANNs can predict the majority of the most severe *gz_lt02* level occurrences: threshold 3 crossings are predicted three times on four occurrences, with the missed prediction referring to a validation event. The validation set comprises only two crossings of the higher threshold and the prediction percentage is 50%, but more data would be necessary to better assess the performance. All the lower threshold crossings are predicted, while some are missed for the intermediate one, and for both the performances on the calibration and validation sets are comparable. The average warning time ranges between approximately 25 and 40 minutes for short-term predictions, while the use of nowcasting information allows to increase the forecast anticipation to approximately 2 hours. The absolute value of the average prediction delay is generally lower than 10 minutes, the only higher value being the -20 minutes delay obtained for ANN_{LL} with respect to the two predicted Threshold 2 crossings in the validation set (i.e. the signalled crossing times are, on average, 20 minutes early with respect to the actual ones). As regards sewer flow predictions, they are again slightly outperformed by level forecasts. This may be due to observed *ml01* flows during rainfall events being less

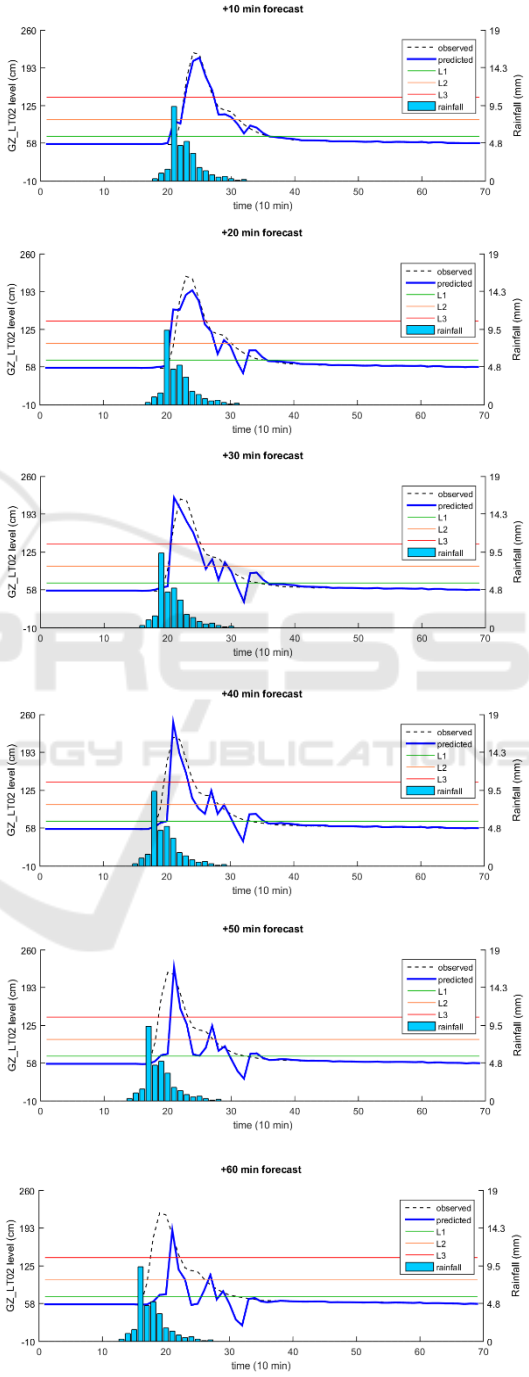

Figure 3: ANN_{LS} envelop of level forecast for a validation event.

regular with respect to those of the VG level. The highest flow threshold crossings are always predicted, even if they occur just once in the calibration events and once in the validation events. The average warning time and prediction delay are comparable to the ones obtained for level forecasts. All models generate some false alerts, especially for the lowest threshold, while never for the highest one.

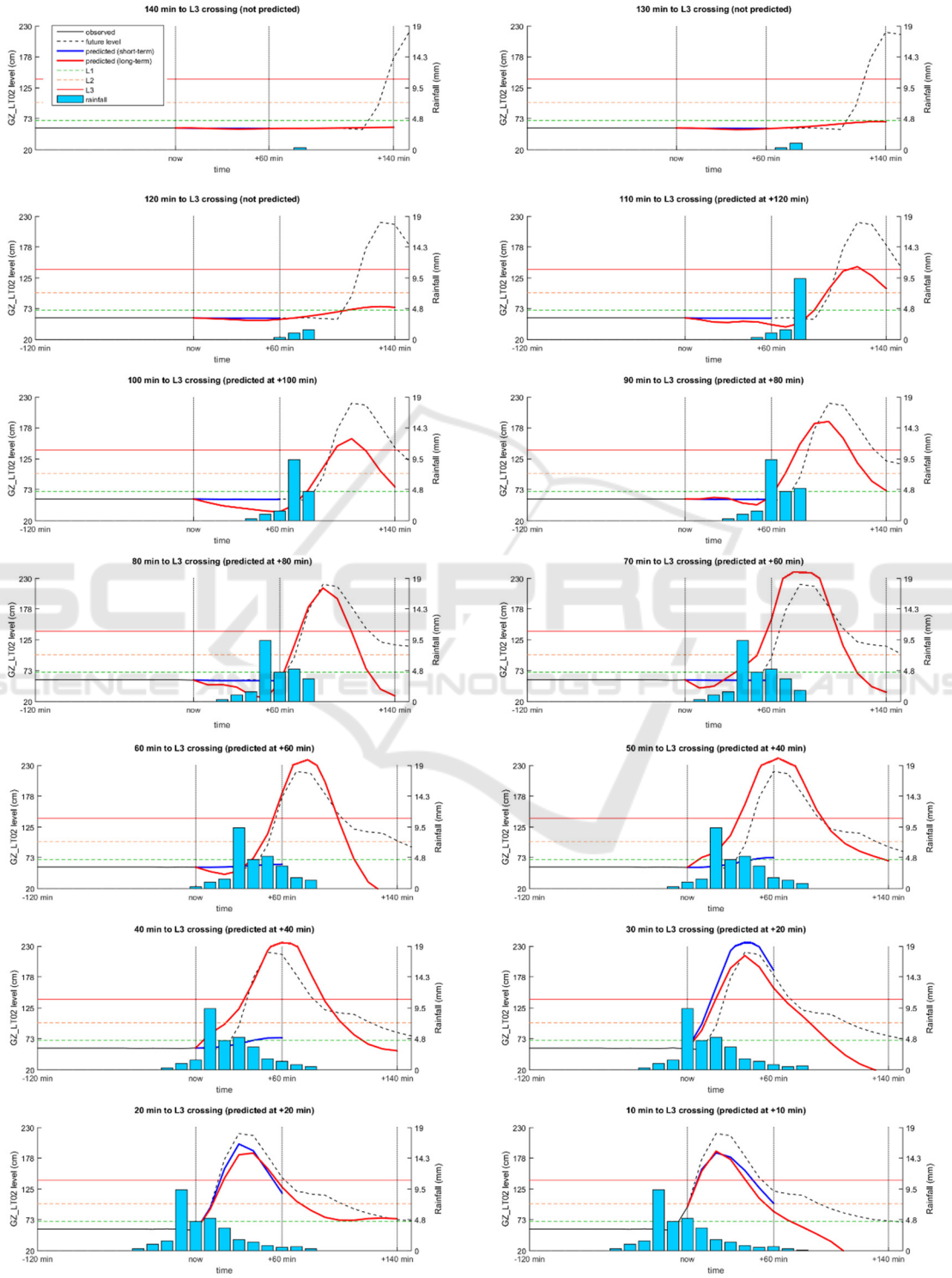

Figure 4: Level 3 crossing prediction efficiency from 140 to 10 minutes before the first occurrence during a validation event.

Some examples of the prediction performance on a severe event in the validation set, during which all the thresholds are crossed, are shown in Figures 3 and 4. Figure 3 shows, for all the short-term prediction horizons, the envelop of the forecasted level vs the observed one. Figure 4 shows, for the same event, a sort of "snap-shot" of the User Interface (UI) from 140 to 10 minutes prior to the first crossing of the L3 threshold. As in the actual UI described in next section, the time axis spans from 120 minutes prior to the current time to 180 minutes after. Measured and forecasted rainfalls and levels are shown. The observed future level is also shown for comparison purpose. As it can be noticed, the first alert is given 110 minutes before the actual crossing, thanks to the long-term predicting ANN (red line), even if the crossing is signalled to occur within 120 minutes. 80 minutes before the crossing, the amount of expected level becomes more reliable. The short-term prediction (blue line) raises above L3 only 30 minutes before the crossing. Indeed, up to 40 minutes before the crossing, the amount of measured rainfall is still quite low, and consequently ANN_{LS} predicts just a small level raise. The considerable rainfall intensity increase that is measured 30 minutes before the crossing is finally allowing ANN_{LS} to predict a steep raise of *gz_lt02* level. This example underlines the importance of nowcasting information, that permits to have alerts of incoming critical events with a reasonable advance.

3.2 User Interface

The DSS was designed to provide a comprehensive view of the sewerage network, with a particular focus on the two key parameters defined in section 2. Thus, a UI was created. Specifically, it was developed as a QGIS plugin, to allow further improvements using georeferenced data. Weights and biases were extracted from the selected ANNs allowing to write real-time running forecast algorithms consisting in in linear algebra operations on matrices. These algorithms, together with all the other necessary scripts running behind the DSS, were developed through the Python language. All measured and processed data are stored in the DSS database. From there, data are picked to be shown in the User Interface. In particular, the UI (Figure 5) shows directly measured quantities (e.g. current values of levels along the VG channel, VF gate openings, flows) together with derived quantities (as for example the estimated CSO downstream *ml01* that, given the difficulty in placing a meter due to morphological issues, was estimated by means of water mass balance between the collector flow and the internal WWTP flow during rainfall events). The UI also can display the results of simulations of the VF channel behaviour using different mitigation strategies, as explained later on. The main section is dedicated to the visualization of the VG levels at *gz_lt02* (blue lines) and *ml01* discharge (orange lines) as recorded for the past 6 hours (continuous lines) and predicted for the next 60 minutes (dashed lines) or 140 minutes (dotted lines). Above the main plot, the current and suggested openings for the 5 operable gates (labelled as Nr.2, Nr.10, Nr.14A, Nr.14B, and Nr.15 in the UI) is also shown. The gate-opening strategy is driven by the measured VG level at *gz_lt02*. The three threshold values defined for the

Figure 5: User Interface in the QGIS plugin.

Figure 6: Real-time Grafana visualization dashboard.

VG level (L1=70 cm, L2=100 cm, L3=140 cm) trigger four different combinations of suggested gate openings (namely “A”, “B”, “C” and “D” in the UI) that are characterized by an increasing quantity of spilled water and storage area usage, resulting in a decreasing discharge into the VG channel until it is completely blocked in case most severe events. The suggested strategy is highlighted in yellow and the current openings are highlighted in green or red, depending on whether they are in accordance or not with the proposed ones, with a 5 cm tolerance. At this first stage, the suggested strategies are based on the long-time experience of the WWTP technicians. However, the “Simulation” section of the UI, below the main plots, embeds a physically-based HEC-RAS hydraulic model of the VF (not discussed here for the sake of brevity) that can be executed between two selected timestamps using past boundary conditions. Thus, by changing the threshold values of the VG level or the suggested gate openings, ex-post analyses can be performed with the final aim of assessing the goodness of the adopted strategies or detecting more efficient parameter combinations.

The described UI, allowing to change the DSS parameters, is thought to be used by expert operators. In addition, for all other operators, a visualization-only UI was developed through the Grafana platform. It allows data visualization on desktop and mobile devices and is composed of three dashboards, the main one showing the current system status (Figure 6), another showing past data in a selected time interval and the last showing “snap-shots” of the main dashboard plots at a selected past timestamp.

4 DISCUSSION

The results presented in Section 3 indicate that the developed DSS is already able to give useful insights to the WWTP operators and to help them in managing potentially critical events.

The real-time monitoring of measured quantities gives useful advice to the operator: when the crossing of a threshold level happens, the flood wave takes some time (approx. 30 to 90 minutes) to reach the overflow point, allowing for a timely intervention to mitigate the risk of overflows. Furthermore, the system status forecast provides operators with additional information, guiding them in taking the proper decision. As an example, if an alert in the UI suggests a specific strategy related to measured *gz_lt02* threshold crossing, but the forecast is showing that level is going to decrease soon after, the operator may decide not to adopt any mitigation strategy. On the contrary, forecasts of incoming critical conditions allow to be ready and possibly anticipate the mitigation manoeuvres. The average warning time is in fact sufficient for operators to be ready to adopt proper risk mitigation strategies. In particular, the most critical events are predicted with an average warning time of approximately 30 minutes based on observed rainfall only, while nowcasting

allows for an alert anticipation greater than 100 minutes. The prediction timing is fairly accurate, in particular for VG level variation, with an average delay almost always lower than 10 minutes. Based on these considerations, the implemented ANNs can be considered helpful tools in the developed DSS.

However, since this is a first stage project, several improvements may be implemented. First, the ANNs performance may be enhanced as long as more data become available, being all collected in the DSS database. Also, different ANN structures may be implemented. Recurrent neural networks as the Long Short-Term Memory (LSTM) ones (Hochreiter and Schmidhuber., 1997) are particularly suited in modelling time series and an attempt could be made using such ANN architecture. Given the DSS structure, such an operation would not be complicated. New ANNs can be trained offline, then if better performances are gained the scripts may be easily adjusted. Moreover, at the current stage it was decided not to use a testing set to evaluate the ANNs performance. The future availability of more records will allow to perform analyses on unseen data.

Another aspect that should be investigated is related to rainfall forecasts. As already said, nowcasting allows to generate alerts with a reasonable advance. However, in the present study measured rainfalls were used also as predicted ones, in a perfect forecast hypothesis. Obviously the actual nowcasting information could be less accurate and the effects on level and flow predictions should be evaluated. This is why it was chosen to keep also the short-term ANNs in the DSS, as they rely on measured data which are not affected by uncertainties.

As regards the risk mitigation strategies, they are currently suggested in the UI based on the level of the receiving channel. The four different gate openings combinations, associated to three VG thresholds levels, have been discussed with the WWTP technicians and at this stage are still based on their long-time experience. However, the hydraulic model integrated in the DSS allows operators to perform ex-post simulations, assessing the effectiveness of the adopted strategy or evaluating the effects of different gate openings or different threshold levels. On this basis, the predefined suggested strategies may be easily changed by expert operators directly in the UI. Future developments will include the integration of multi-objective optimization functionalities in the system, benefitting from the detailed information that will become available in the database, in order to face conflicting objectives as the need of sending as much water as possible to the receiving body while minimizing the chance of overflows, eventually obtaining case-specific threshold levels and gate openings combinations. For example, the premature filling of the storage area may produce negative effects during successive intense rainfalls, and unnecessary lateral spills may result in exceeding the allowed discharge in surrounding rural channels. Such improvements could be achieved by integrating real-time execution of the hydraulic model, performing simulations based on forecasted variables and different sets of threshold levels and gate openings: optimization algorithms will eventually determine the best combination to face the incoming events. Finally, when a considerable amount of available data will allow to accurately understand and model all the hydraulic processes, the VF gates could be provided with automated actuators in order to implement a Real Time Control System.

5 CONCLUSIONS

The case study presented in this paper illustrates a smart infrastructure project, specifically the design of a DSS platform able to provide real-time monitoring, weather nowcasting and forecasts on the status of some key variables, in the context of managing a medium-size city wastewater treatment plant. With respect to the state of the art, a simplified approach for modelling hydraulic variables based on Artificial Neural Networks is proposed.

Data are acquired with a 10-minute frequency from a network of sensors and are stored in a single database that hosts heterogeneous variables, some of which are used to perform run-time analyses using ANNs. These are trained based on past events and can be updated as more data become available. The update procedure can be performed “offline”, this being an important feature of the system design as, once implemented and calibrated under certain assumptions, it would be possible to improve the performance and/or adapt the algorithms to different conditions without any substantial revision of the software architecture. Moreover, an automated update procedure can be foreseen in future improvements of the proposed system: a script reading the database with an imposed frequency – e.g. twice a year – could then process the new acquired data, add them to the training dataset and perform again the training procedure, replacing the matrices if better results are gained.

The DSS was implemented to provide support for a WWTP with the twofold objective of monitoring the inlet flow to the plant and reducing the chance of

overflow during severe rainfall events. The system management is further aided by forecasts shown in the plot window, which provide additional information about the forthcoming behaviour of key variables, as predicted by ANNs.

When dealing with Smart City projects, several challenges arise. It is important to lower the design and operational costs to increase the probability of implementation. The handling of heterogeneous data from multiple sources, the analysis of Big Data and security-related issues are also to be considered (Silva et al., 2018). The proposed approach, fulfilling these requirements, is a valuable step in guaranteeing safety in a Smart City context and can be in principle replicated and applied in all those settings where measurements from different sensors over large areas, meteorological data, and in general any quantitative information needs to be processed to provide synthetic outputs for the final user.

ACKNOWLEDGEMENTS

The study presented in this paper is part of the INNOVA EFD3 research project financed by A2A Ciclo Idrico S.p.A.

REFERENCES

Bellon, A., Zawadzki, I., Kilambi, A., Lee, H.C., Lee, Y.H. and Lee, G., 2010. “McGill algorithm for precipitation nocasting by Lagrangian extrapolation (MAPLE) applied to the South Korean radar network. Part I: Sensitiity studies of the Variational Echo Tracking (VET) technique.” Asia-Pacific Journal of Atmospheric Scences 46(3): 369-381.

Botturi, A., Gozde Ozbayram, E., Tondera, K., Gilbert, N.I., Rouault, P., Caradot, N., Gutierrez, O., Daneshgar, S., Frison, N., Akyol, C., Foglia, A., Eusebi, A.L. and Fatone, F., 2020. “Combined sewer overflows: A critical review on best practice and innovative solutions to mitigate impacts on environment and human health”. Critical Reviews in Environmental Science and Technology, 1-34.

Campisano, A., Creaco, E., and Modica, C., 2016. “Application of real-time control techniques to reduce water volume discharges from quality-oriented CSO devices”. Journal of Environmental Engineering, 142(1), 04015049 1-8.

Carbone, M., Garofalo, G., and Piro, P., 2014. “Decentralized real time control in combined sewer system by using smart objects”. Procedia Engineering, 89, 473–478.

Clark, M.P., Bierkens, M.F.P., Samaniego, L., Woods, R.A., Uijlenhoet, R., Bennett, K.E., Pauwels, V.R.N., Cai, X., Wood, A. and Peters-Lidard, C.D., 2017. “The evolution of process-based hydrologic models: historical challenges and the collective quest for physical realism.” Hydrology and Earth System Sciences 21: 3427-3440.

Hochreiter, S. and Schmidhuber, J., 1997. “Long short-term memory”. Neural computation, 9(8), 1735-1780.

Jeong, J., Kannan, N., Arnold, J., Glick, R., Gosselink, L. and Srinivasan, R., 2010. “Development and integration of sub-hourly rainfall–runoff modeling capability within a watershed model”. Water Resources Management, 24(15): 4505-4527.

Lee, H.C., Lee, Y.H., Ha, J.C., Chang, D.E., Bellon, A., Zawadzki, I. and Lee, G., 2010. “McGill Algorithm for Precipitation Nowcasting by Lagrangian Extrapolation (MAPLE) applied to the South Korean radar network. Part II: Real-time verification for the summer season.” Asia-Pacific Journal of Atmospheric Sciences 46(3): 383-391.

Maier, H. R., Jain, A., Dandy G.C. and. Sudheer, K.P., 2010. “Methods used for the development of neural networks for the prediction of water resource variables in river systems: Current status and future directions.” Environmental modelling & software 25(8): 891-909.

Mandapaka, P.V., Germann, U., Panziera, L. and Hering, A., 2012. “Can Lagrangian extrapolation of radar fields be used for precipitation nowcasting over complex Alpine orography?” Weather and forecasting 27(1): 28-49.

Panziera, L., Germann, U. Gabella., M. and Mandapaka, P.V., 2011. “NORA –Nowcasting of Orographic Rainfall by means of Analogues.” Quarterly Journal of the Royal Meteorological Society 137(661): 2106-2123.

Park, T., and Kim, H.A., 2013. “A data warehouse-based decision support system for sewer infrastructure management.” Automation in Construction 30: 37-49.

Pereira, A., Pinho, J.L.S., Vieira, J.M.P., Faria, R., and Costa, C., 2019. “Improving operational management of wastewater systems. A case study.” Water Science and Technology 80(1): 173-183.

Rao, M. 2015. “A performance measurement application for a wastewater treatment plant.” International Journal of Services and Standards 10(3): 134-147.

Rechdaoui-Guérin, S., Bersinger, T., Bareille, G., Pigop, T., Le Hécho, I., Azimi, S. and Rocher, V., 2018. “Monitoring the quality of effluents in a unitary sanitation network” Technique-Sciences-Methodes 113: 77-90.

Silva, B. N., Khan, M., and Han, K., 2018. “Towards sustainable smart cities: A review of trends, architectures, components, and open challenges in smart cities”. Sustainable Cities and Society, 38: 697-713.

US EPA. (2018). Smart data infrastructure for wet weather control and decision support. EPA 830-B-17-004.

Wilson, J.W., Crook, N.A., Mueller, C.K., Sun, J. and Dixon, M., 1998. “Nowcasting thunderstorms: A status report.” Bulletin of the American Meteorological Society 79(10): 2079-2100.